

Lagrangian schemes with topology changes
and well balanced techniques for the solution
of hyperbolic partial differential equations

Elena Gaburro

DICAM, University of Trento, Italy

5 November 2020

GOAL: preserving at **discrete level**
the physical properties of the **continuum model**

- **Lagrangian schemes (ALE)** → **Galilean and rotational invariance**
Better track of contact discontinuities and material interfaces, reduced errors on convective terms
Applications: geophysics, magnetohydrodynamics, continuum mechanics
- **Well balanced schemes (WB)** → **Equilibria preservation**
More accurate simulation of small perturbations
Applications: astrophysics from Newtonian E+G to relativistic GRMHD and FO-CCZ4
- **ALE + WB**
Applications: Euler equations with gravity (E+G)

Hyperbolic partial differential equations

$$\partial_t \mathbf{Q} + \nabla \cdot \mathbf{F}(\mathbf{Q}) + \mathbf{B}(\mathbf{Q}) \cdot \nabla \mathbf{Q} = \mathbf{S}(\mathbf{Q}), \quad \mathbf{x} \in \Omega \subset \mathbb{R}^3, \quad t \in \mathbb{R}_0^+$$

$\mathbf{Q} = (q_1, q_2, \dots, q_\nu) \in \Omega_Q \quad \rightarrow$ vector of **conserved variables**
(densities, velocities, magnetic field, energy, ...)

$\mathbf{F} = (\mathbf{f}, \mathbf{g}, \mathbf{h}) \quad \rightarrow$ **non linear** flux

$\mathbf{B} = (\mathbf{B}_1, \mathbf{B}_2, \mathbf{B}_3) \quad \rightarrow$ **non conservative** terms

$\mathbf{S} \quad \rightarrow$ **non linear** source term

Multiphysics:

Shallow water, Euler (HD), multiphase, magneto-hydrodynamics (MHD),
unified models for continuum mechanics (GPR),
general relativity : GRHD, GRMHD, Einstein field equations (CCZ4) ...

Direct ALE WB FV-DG for hyperbolic PDEs

Well balanced Arbitrary-Lagrangian-Eulerian Finite Volume and Discontinuous Galerkin schemes for nonlinear hyperbolic equations

$\mathbf{Q} = (q_1, q_2, \dots, q_\nu) \in \Omega_Q \quad \rightarrow \quad$ vector of **conserved variables**
(densities, velocities, magnetic field, energy, ...)

$\mathbf{F} = (\mathbf{f}, \mathbf{g}, \mathbf{h}) \quad \rightarrow \quad$ **non linear** flux

$\mathbf{B} = (\mathbf{B}_1, \mathbf{B}_2, \mathbf{B}_3) \quad \rightarrow \quad$ **non conservative** terms

$\mathbf{S} \quad \rightarrow \quad$ **non linear** source term

Multiphysics:

Shallow water, **Euler** (HD), **multiphase**, **magneto-hydrodynamics** (MHD),
unified models for **continuum mechanics** (GPR),
general **relativity** : GRHD, GRMHD, **Einstein** field equations (CCZ4) ...

Direct ALE WB **FV-DG** for hyperbolic PDEs

High order Finite Volume and Discontinuous Galerkin schemes
unified framework \rightarrow FV robustness + DG resolution

$\mathbf{Q} = (q_1, q_2, \dots, q_\nu) \in \Omega_Q \quad \rightarrow$ vector of **conserved variables**
(densities, velocities, magnetic field, energy, ...)

$\mathbf{F} = (\mathbf{f}, \mathbf{g}, \mathbf{h}) \quad \rightarrow$ **non linear** flux

$\mathbf{B} = (\mathbf{B}_1, \mathbf{B}_2, \mathbf{B}_3) \quad \rightarrow$ **non conservative** terms

$\mathbf{S} \quad \rightarrow$ **non linear** source term

Multiphysics:

Shallow water, Euler (HD), multiphase, magneto-hydrodynamics (MHD),
unified models for **continuum mechanics** (GPR),
general **relativity** : GRHD, GRMHD, **Einstein** field equations (CCZ4) ...

Direct ALE FV-DG for hyperbolic PDEs

Direct Arbitrary-Lagrangian-Eulerian schemes

reduce convective errors + interface tracking + higher quality meshes

$\mathbf{Q} = (q_1, q_2, \dots, q_\nu) \in \Omega_Q \quad \rightarrow \quad$ vector of **conserved variables**
(densities, velocities, magnetic field, energy, ...)

$\mathbf{F} = (\mathbf{f}, \mathbf{g}, \mathbf{h}) \quad \rightarrow \quad$ **non linear** flux

$\mathbf{B} = (\mathbf{B}_1, \mathbf{B}_2, \mathbf{B}_3) \quad \rightarrow \quad$ **non conservative** terms

$\mathbf{S} \quad \rightarrow \quad$ **non linear** source term

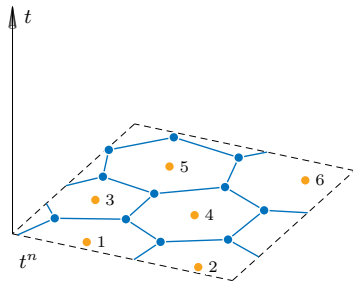
Multiphysics:

Shallow water, **Euler** (HD), **multiphase**, **magneto-hydrodynamics** (MHD),
unified models for **continuum mechanics** (GPR),
general **relativity** : GRHD, GRMHD, **Einstein** field equations (CCZ4) ...

ALE methods: moving domain discretization

Unstructured **moving meshes**: made of triangles or polygons

connected in **space** and **time**
→ **space-time control volume**

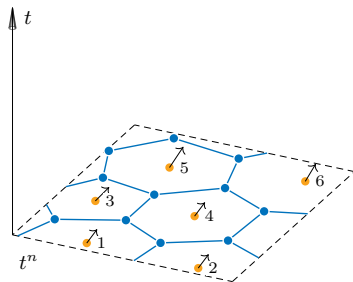


ALE methods: moving domain discretization

Unstructured **moving meshes**: made of triangles or polygons

connected in **space** and **time**

→ **space-time control volume**

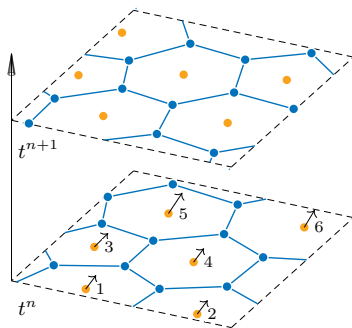


ALE methods: moving domain discretization

Unstructured **moving meshes**: made of triangles or polygons

connected in **space** and **time**

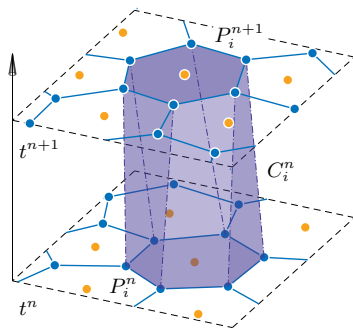
→ **space-time control volume**



ALE methods: moving domain discretization

Unstructured **moving meshes**: made of triangles or polygons

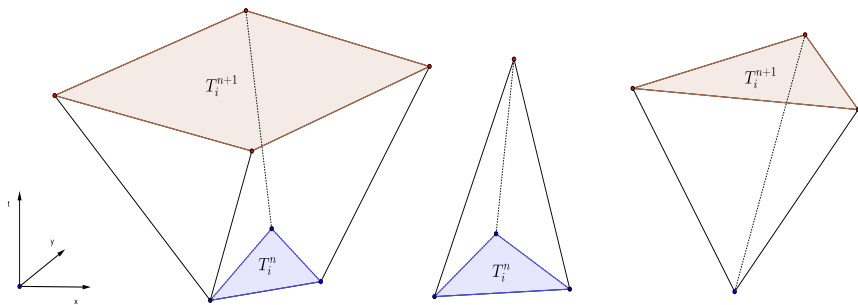
connected in **space** and **time**
→ **space-time control volume**



ALE methods: moving domain discretization

Degenerated *crazy* control volumes

Change of shape, new and dead elements



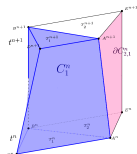
Direct ALE FV-DG scheme

The governing PDE is reformulated in a space-time divergence form

$$\boxed{\tilde{\nabla} \cdot \tilde{\mathbf{F}} = \mathbf{S}} \quad \text{with } \tilde{\nabla} = (\partial_x, \partial_y, \partial_z, \partial_t)^T \text{ and } \tilde{\mathbf{F}} = (\mathbf{F}, \mathbf{Q})$$

and is **integrated in space and time** against a set of **test functions** φ_k

$$\int_{C_i^n} \varphi_k \tilde{\nabla} \cdot \tilde{\mathbf{F}} \, dx dt = \int_{C_i^n} \varphi_k \mathbf{S} \, dx dt$$



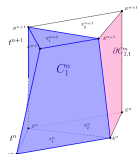
Direct ALE FV-DG scheme

The governing PDE is reformulated in a space-time divergence form

$$\boxed{\tilde{\nabla} \cdot \tilde{\mathbf{F}} = \mathbf{S}} \quad \text{with } \tilde{\nabla} = (\partial_x, \partial_y, \partial_z, \partial_t)^T \text{ and } \tilde{\mathbf{F}} = (\mathbf{F}, \mathbf{Q})$$

and is **integrated in space and time** against a set of **test functions** φ_k

$$\int_{C_i^n} \varphi_k \tilde{\nabla} \cdot \tilde{\mathbf{F}} \, dxdt = \int_{C_i^n} \varphi_k \mathbf{S} \, dxdt$$



Then using the Gauss theorem

ALE FV-DG scheme i.e. ALE $P_N P_M$ scheme

$$\int_{\partial C_i^n} \varphi_k \tilde{\mathbf{F}} \cdot \tilde{\mathbf{n}} \, dSdt - \int_{C_i^n} \tilde{\nabla} \varphi_k \cdot \tilde{\mathbf{F}} \, dxdt = \int_{C_i^n} \varphi_k \mathbf{S} \, dxdt$$

Direct ALE FV-DG scheme

ALE FV-DG scheme

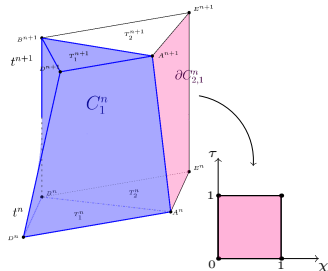
$$\int_{\partial C_i^n} \varphi_k \tilde{\mathbf{F}} \cdot \tilde{\mathbf{n}} dS dt - \int_{C_i^n} \tilde{\nabla} \varphi_k \cdot \tilde{\mathbf{F}} dx dt = \int_{C_i^n} \varphi_k \mathbf{S} dx dt$$

$$\int_{T_i^{n+1}} \varphi_k \mathbf{Q}_i^{n+1} dx = \int_{T_i^n} \varphi_k \mathbf{Q}_i^n dx - \int_{\partial C_{ij}^n} \varphi_k \mathcal{F}(\mathbf{q}_h^-, \mathbf{q}_h^+) \cdot \tilde{\mathbf{n}} dS dt$$

$$+ \int_{C_i^n} \tilde{\nabla} \varphi_k \cdot \tilde{\mathbf{F}}(\mathbf{q}_h) dx dt$$

$$+ \int_{C_i^n} \varphi_k \tilde{\mathbf{S}}(\mathbf{q}_h) dx dt$$

$$\varphi_k = 1, \mathbf{Q}_i = \text{constant} \rightarrow \mathbf{FV}$$



Direct ALE FV-DG scheme

ALE FV-DG scheme

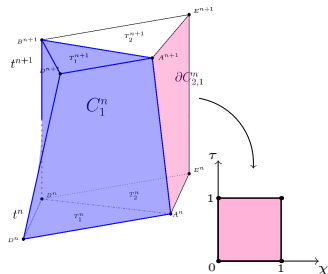
$$\int_{\partial C_i^n} \varphi_k \tilde{\mathbf{F}} \cdot \tilde{\mathbf{n}} dS dt - \int_{C_i^n} \tilde{\nabla} \varphi_k \cdot \tilde{\mathbf{F}} dx dt = \int_{C_i^n} \varphi_k \mathbf{S} dx dt$$

$$\int_{T_i^{n+1}} \varphi_k \mathbf{Q}_i^{n+1} dx = \int_{T_i^n} \varphi_k \mathbf{Q}_i^n dx - \int_{\partial C_{ij}^n} \varphi_k \mathcal{F}(\mathbf{q}_h^-, \mathbf{q}_h^+) \cdot \tilde{\mathbf{n}} dS dt$$

$$+ \int_{C_i^n} \tilde{\nabla} \varphi_k \cdot \tilde{\mathbf{F}}(\mathbf{q}_h) dx dt$$

$$+ \int_{C_i^n} \varphi_k \tilde{\mathbf{S}}(\mathbf{q}_h) dx dt$$

$$\varphi_k = \text{poly}, \quad \mathbf{Q}_i^{n/n+1} = \sum_{l=1}^{\mathcal{N}} \varphi_l(\mathbf{x}) \hat{\mathbf{u}}_{l,i}^{n/n+1} \quad \rightarrow \quad \mathbf{DG}$$



Direct ALE FV-DG scheme

ALE FV-DG scheme

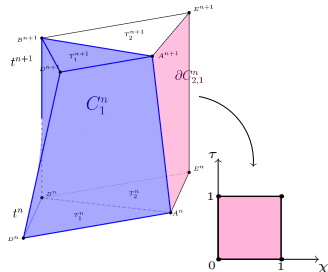
$$\int_{\partial C_i^n} \varphi_k \tilde{\mathbf{F}} \cdot \tilde{\mathbf{n}} dS dt - \int_{C_i^n} \tilde{\nabla} \varphi_k \cdot \tilde{\mathbf{F}} dx dt = \int_{C_i^n} \varphi_k \mathbf{S} dx dt$$

$$\int_{T_i^{n+1}} \varphi_k \mathbf{Q}_i^{n+1} dx = \int_{T_i^n} \varphi_k \mathbf{Q}_i^n dx - \int_{\partial C_{ij}^n} \varphi_k \mathcal{F}(\mathbf{q}_h^-, \mathbf{q}_h^+) \cdot \tilde{\mathbf{n}} dS dt$$

$$+ \int_{C_i^n} \tilde{\nabla} \varphi_k \cdot \tilde{\mathbf{F}}(\mathbf{q}_h) dx dt$$

$$+ \int_{C_i^n} \varphi_k \tilde{\mathbf{S}}(\mathbf{q}_h) dx dt$$

ALE Numerical Flux: Riemann solver



ALE numerical flux

$\mathcal{F}(\mathbf{q}_h^-, \mathbf{q}_h^+) \cdot \tilde{\mathbf{n}}$ represents the ALE numerical flux between two neighbors across the intermediate space–time lateral surface ∂C_{ij}^n

Example: **Rusanov** –type ALE scheme

$$\mathcal{F}(\mathbf{q}_h^-, \mathbf{q}_h^+) \cdot \tilde{\mathbf{n}} = \frac{1}{2} \left(\tilde{\mathbf{F}}(\mathbf{q}_h^+) + \tilde{\mathbf{F}}(\mathbf{q}_h^-) \right) \cdot \tilde{\mathbf{n}}_{ij} - \frac{1}{2} \lambda_{max} (\mathbf{q}_h^+ - \mathbf{q}_h^-)$$

- $\mathbf{A}_n^V(\mathbf{Q})$ is the **ALE Jacobian matrix** w.r.t. the normal direction in space, i.e.

$$\mathbf{A}_n^V(\mathbf{Q}) = \left(\sqrt{\tilde{n}_x^2 + \tilde{n}_y^2} \right) \left[\frac{\partial \mathbf{F}}{\partial \mathbf{Q}} \cdot \mathbf{n} - (\mathbf{V} \cdot \mathbf{n}) \mathbf{I} \right], \quad \mathbf{n} = \frac{(\tilde{n}_x, \tilde{n}_y)^T}{\sqrt{\tilde{n}_x^2 + \tilde{n}_y^2}}$$

with \mathbf{I} representing the identity matrix and $\mathbf{V} \cdot \mathbf{n}$ denoting the local normal mesh velocity.

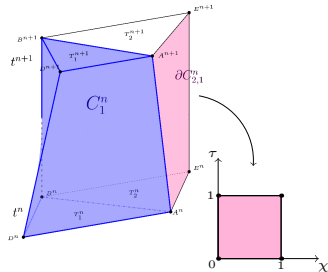
Direct ALE FV-DG scheme

ALE FV-DG scheme

$$\int_{\partial C_i^n} \varphi_k \tilde{\mathbf{F}} \cdot \tilde{\mathbf{n}} dS dt - \int_{C_i^n} \tilde{\nabla} \varphi_k \cdot \tilde{\mathbf{F}} dx dt = \int_{C_i^n} \varphi_k \mathbf{S} dx dt$$

$$\begin{aligned} \int_{T_i^{n+1}} \varphi_k \mathbf{Q}_i^{n+1} dx &= \int_{T_i^n} \varphi_k \mathbf{Q}_i^n dx - \int_{\partial C_{ij}^n} \varphi_k \mathcal{F}(\mathbf{q}_h^-, \mathbf{q}_h^+) \cdot \tilde{\mathbf{n}} dS dt \\ &+ \int_{C_i^n} \tilde{\nabla} \varphi_k \cdot \tilde{\mathbf{F}}(\mathbf{q}_h) dx dt \\ &+ \int_{C_i^n} \varphi_k \tilde{\mathbf{S}}(\mathbf{q}_h) dx dt \end{aligned}$$

High order polynomial in space and time



FV high order in space: CWENO

$$\mathbf{FV} \quad \mathbf{Q}_i^n \longrightarrow \mathbf{w}_h(\mathbf{x}, t^n) = \sum_{l=1}^{\mathcal{M}} \psi_l(\mathbf{x}) \hat{\mathbf{w}}_{l,i}^n \quad \mathcal{M} = \frac{1}{d!} \prod_{k=1}^d (M + k)$$

High order **polynomial** in space

impose **integral conservation** on each element of the stencil

$$\frac{1}{|T_j^n|} \int_{T_j^n} \psi_l(\mathbf{x}) \hat{\mathbf{w}}_{l,i}^{n,s} = \mathbf{Q}_j^n, \quad \forall T_j^n \in S_i^n$$

and compute their **nonlinear combination**

$$\hat{\mathbf{w}}_{l,i}^n = \sum_s \omega_s \hat{\mathbf{w}}_{l,i}^{n,s}, \quad \text{with } \omega_s \text{ nonlinear CWENO weights}$$

CWENO:

one central big stencil and
several smaller stencils

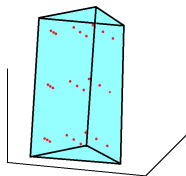
DG high order in space

$$\mathbf{DG} \quad \mathbf{Q}_i^n \rightarrow \mathbf{u}_h(\mathbf{x}, t^n) = \sum_{\ell=1}^{\mathcal{N}} \varphi_{\ell}(\mathbf{x}, t) \hat{\mathbf{u}}_{\ell}^n \quad \mathcal{N} = \frac{1}{d!} \prod_{k=1}^d (N + k)$$

$\varphi(\mathbf{x}, t) \rightarrow$ **Modal basis** : hierarchical Dubiner-type high order polynomial functions in **space** and **moving in time**



$$\begin{aligned} \left(\int_{T_i^{n+1}} \varphi_k \varphi_l d\mathbf{x} \right) \hat{\mathbf{u}}_i^{n+1} &= \left(\int_{T_i^n} \varphi_k \varphi_l d\mathbf{x} \right) \hat{\mathbf{u}}_i^n - \int_{\partial C_{ij}^n} \varphi_k \mathcal{F}(\mathbf{q}_h^-, \mathbf{q}_h^+) \cdot \tilde{\mathbf{n}} dS dt \\ &+ \int_{C_i^n} \tilde{\nabla} \varphi_k \cdot \tilde{\mathbf{F}}(\mathbf{q}_h) d\mathbf{x} dt + \int_{C_i^n} \tilde{\mathbf{S}}(\mathbf{q}_h) d\mathbf{x} dt \end{aligned}$$



High order in time: ADER

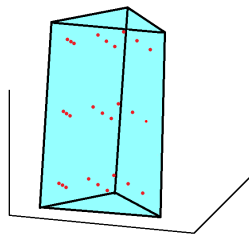
High order in TIME \rightarrow **ADER** one-step **local** Galerkin predictor

$$\mathbf{q}_h(\mathbf{x}, t) = \sum_{l=1}^{\mathcal{L}} \theta_l(\mathbf{x}, t) \hat{\mathbf{q}}_{l,i}^n \rightarrow \text{Picard iteration}$$

Integral version of the PDE

$$\int_{T_i^n} \theta_k(\mathbf{q}_h - \mathbf{w}_h) - \int_{C_i^n} \frac{\partial \theta_k}{\partial t} \mathbf{q}_h + \int_{C_i^n} \theta_k \nabla \cdot \mathbf{F}(\mathbf{q}_h) = \int_{C_i^n} \theta_k \mathbf{S}(\mathbf{q}_h)$$

- $\theta_l(\mathbf{x}, t) \rightarrow$ **modal** basis functions
in **space** and **time**
- $\mathcal{L} = \frac{1}{d!} \prod_{k=1}^{d+1} (M + k)$



High order in time: ADER

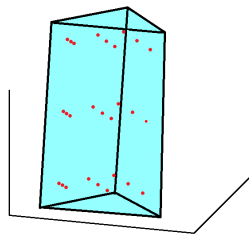
High order in TIME \rightarrow **ADER** one-step **local** Galerkin predictor

$$\mathbf{q}_h(\mathbf{x}, t) = \sum_{l=1}^{\mathcal{L}} \theta_l(\mathbf{x}, t) \hat{\mathbf{q}}_{l,i}^n \rightarrow \text{Picard iteration}$$

Integral version of the PDE

$$\int_{T_i^n} \theta_k(\mathbf{q}_h - \mathbf{u}_h) - \int_{C_i^n} \frac{\partial \theta_k}{\partial t} \mathbf{q}_h + \int_{C_i^n} \theta_k \nabla \cdot \mathbf{F}(\mathbf{q}_h) = \int_{C_i^n} \theta_k \mathbf{S}(\mathbf{q}_h)$$

- $\theta_l(\mathbf{x}, t) \rightarrow$ **modal** basis functions
in **space** and **time**
- $\mathcal{L} = \frac{1}{d!} \prod_{k=1}^{d+1} (M + k)$



High order in time: ADER vs RK

ADER: one-step predictor

- Completely **local** procedure suitable for **efficient parallelization**

Error analysis: Modified equation $\partial_t q + a \partial_x q = \sum_{\ell} e_{\ell} \frac{\partial q^{\ell}}{\partial x^{\ell}}$, $c = \frac{\Delta t}{\Delta x} \leq 1$

ADER $\mathcal{O}4$

$$e_{1,2,3,4} = 0, e_5 = \frac{a \Delta x^4}{120} (c^2 - 1)(c^2 - 4)$$

$$e_6 = \frac{a \Delta x^5}{144} c (c^2 - 1)(c^2 - 4)$$

Runge-Kutta $\mathcal{O}4$

$$e_{1,2,3,4} = 0, e_5 = \frac{a \Delta x^4}{120} (c - \sqrt{2})^2 (c + \sqrt{2})^2$$

$$e_6 = \frac{a \Delta x^5}{144} c^5$$

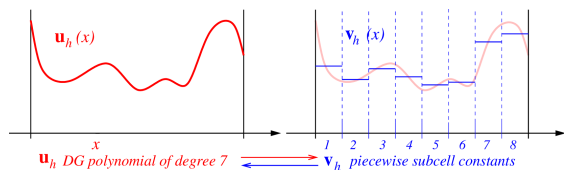
i

DG: A posteriori sub-cell FV limiter

Problem → close to discontinuities Gibbs phenomenon occurs

Solution → use FV in their vicinity without destroy the sub-cell resolution, and keep high accuracy everywhere else

- Projection DG → FV
- A posteriori admissibility criteria
- FV scheme on troubled cells
- Reconstruction FV → DG



$$n_{\text{subcells}} \leq (2N + 1)^d$$

$$\text{because } CFL_{\text{DG}} < \frac{1}{(2N+1)^d} \rightarrow CFL_{\text{FVsubcells}} < 1$$

Degenerated and sliver elements

- ★ **1st step:** Build space-time connectivity
- ★ **2nd step:** Adapt $P_N P_M$ scheme
 - Predictor
 - Corrector

Degenerated and sliver elements

- ★ **1st step:** Build space-time connectivity
- ★ **2nd step:** Adapt $P_N P_M$ scheme
 - Predictor
 - Corrector

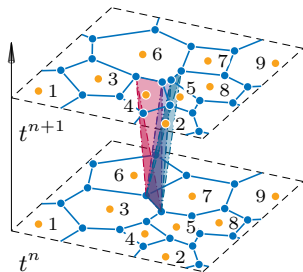
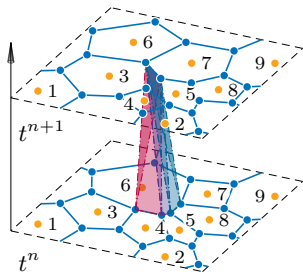
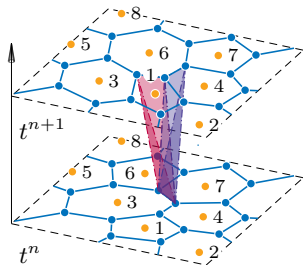
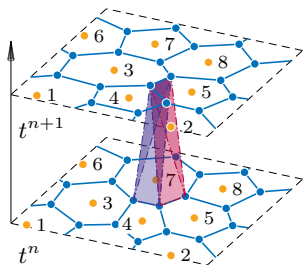
Degenerated and sliver elements

- ★ **1st step:** Build space-time connectivity
- ★ **2nd step:** Adapt $P_N P_M$ scheme
 - Predictor
 - Corrector

Degenerated and sliver elements

- ★ **1st step:** Build space-time connectivity
- ★ **2nd step:** Adapt $P_N P_M$ scheme
 - Predictor
 - Corrector

Consecutive sliver elements



Sliver elements: high order in time

$$\mathbf{q}_h(\mathbf{x}, t) = \sum_{l=1}^{\mathcal{L}} \theta_l(\mathbf{x}, t) \hat{\mathbf{q}}_{l,i}^n \rightarrow \boxed{-\int_{C_i^n} \mathbf{q}_h \frac{\partial \theta_k}{\partial t} + \int_{T_i^n} \theta_k (\mathbf{q}_h - \mathbf{u}_h)} + \int_{C_i^n} \theta_k \nabla \cdot \mathbf{F}(\mathbf{q}_h) = \int_{C_i^n} \theta_k \mathbf{S}(\mathbf{q}_h)$$

Sliver elements: high order in time

$$\mathbf{q}_h(\mathbf{x}, t) = \sum_{l=1}^{\mathcal{L}} \theta_l(\mathbf{x}, t) \hat{\mathbf{q}}_{l,i}^n \rightarrow \boxed{-\int_{C_i^n} \mathbf{q}_h \frac{\partial \theta_k}{\partial t} + \int_{T_i^n} \theta_k (\mathbf{q}_h - \mathbf{u}_h)} + \int_{C_i^n} \theta_k \nabla \cdot \mathbf{F}(\mathbf{q}_h) = \int_{C_i^n} \theta_k \mathbf{S}(\mathbf{q}_h)$$

$$\boxed{\implies} = - \int_{C_i^n} \mathbf{q}_h \frac{\partial \theta_k}{\partial t} + \int_{\partial C_i^n} \theta_k \mathbf{q}_h \cdot \tilde{\mathbf{n}}$$

Sliver elements: high order in time

$$\mathbf{q}_h(\mathbf{x}, t) = \sum_{l=1}^{\mathcal{L}} \theta_l(\mathbf{x}, t) \hat{\mathbf{q}}_{l,i}^n \rightarrow \boxed{-\int_{C_i^n} \mathbf{q}_h \frac{\partial \theta_k}{\partial t} + \int_{T_i^n} \theta_k (\mathbf{q}_h - \mathbf{u}_h^?)} + \int_{C_i^n} \theta_k \nabla \cdot \mathbf{F}(\mathbf{q}_h) = \int_{C_i^n} \theta_k \mathbf{S}(\mathbf{q}_h)$$

$$\boxed{\Rightarrow} = - \int_{C_i^n} \mathbf{q}_h \frac{\partial \theta_k}{\partial t} + \int_{\partial C_i^n} \theta_k \mathbf{q}_h \cdot \tilde{\mathbf{n}} \\ - \int_{C_i^n} \mathbf{q}_h^- \frac{\partial \theta_k}{\partial t} + \int_{\partial C_i^n} \theta_k (\mathbf{q}_h^+ - \mathbf{q}_h^-) \cdot \tilde{\mathbf{n}}^-$$

\mathbf{q}_h^+ \rightarrow blue sub volumes, known

\mathbf{q}_h^- \rightarrow red sub volume, unknown

Space-time predictor for sliver elements

$$-\int_{C_i^n} \mathbf{q}_h^- \frac{\partial \theta_k}{\partial t} + \int_{\partial C_i^n} \theta_k (\mathbf{q}_h^+ - \mathbf{q}_h^-) \cdot \tilde{\mathbf{n}}^- + \int_{C_i^n} \theta_k \nabla \cdot \mathbf{F}(\mathbf{q}_h^-) = \int_{C_i^n} \theta_k \mathbf{S}(\mathbf{q}_h^-)$$

Sliver elements: flux update

- Quadrature points

Sliver elements: flux update

- Flux computation
(from blue to red)
- Flux **redistribution**
(from red to 1st blue)

Sliver elements: flux update

- Flux computation
(from blue to red)
- Flux **redistribution**
(from red to 1st blue)

$$|T_S^{n+1}| \mathbf{Q}_S^{n+1} = |T_S^n| \mathbf{Q}_S^n - \mathcal{F}(\mathbf{q}_h^S, \mathbf{q}_h^+) \cdot \tilde{\mathbf{n}}$$

Sliver elements: flux update

- Flux computation
(from blue to red)
- Flux **redistribution**
(from red to 1st blue)

$$0 \cdot \mathbf{Q}_S^{n+1} = 0 \cdot \mathbf{Q}_S^n - \mathcal{F}(\mathbf{q}_h^S, \mathbf{q}_h^+) \cdot \tilde{\mathbf{n}}$$

Sliver elements: flux update

- Flux computation
(from blue to red)
- Flux **redistribution**
(from red to 1st blue)

$$\mathbf{0} = \mathbf{0} - \mathcal{F}(\mathbf{q}_h^S, \mathbf{q}_h^+) \cdot \tilde{\mathbf{n}}$$

Sliver elements: flux update

- Flux computation
(from blue to red)
- Flux **redistribution**
(from red to 1st blue)

$$\mathbf{0} = \mathbf{0} - \mathcal{F}(\mathbf{q}_h^S, \mathbf{q}_h^+) \cdot \tilde{\mathbf{n}}$$
$$|T_i^{n+1}| \mathbf{Q}_i^{n+1} = |T_i^n| \mathbf{Q}_i^n - \mathcal{F}(\mathbf{q}_h^i, \mathbf{q}_h^+) \cdot \tilde{\mathbf{n}}$$

Sliver elements: flux update

- Flux computation
(from blue to red)
- Flux **redistribution**
(from red to 1st blue)

$$\begin{aligned}
 \mathbf{0} &= \mathbf{0} - \mathcal{F}(\mathbf{q}_h^S, \mathbf{q}_h^+) \cdot \tilde{\mathbf{n}} \\
 + \quad |T_i^{n+1}| \mathbf{Q}_i^{n+1} &= |T_i^n| \mathbf{Q}_i^n - \mathcal{F}(\mathbf{q}_h^i, \mathbf{q}_h^+) \cdot \tilde{\mathbf{n}} \\
 \hline
 = \quad |T_i^{n+1}| \mathbf{Q}_i^{n+1} &= |T_i^n| \mathbf{Q}_i^n - \mathcal{F}(\mathbf{q}_h^i, \mathbf{q}_h^+) \cdot \tilde{\mathbf{n}} - \mathcal{F}(\mathbf{q}_h^S, \mathbf{q}_h^+) \cdot \tilde{\mathbf{n}}
 \end{aligned}$$

High order Lagrangian trajectories for generators

Generators trajectories

$$\mathbf{x}_{\text{gen}}^{n+1} = \mathbf{x}_{\text{gen}}^n + \Delta t \mathbf{v}(\mathbf{x}_{\text{gen}}^n)$$

High order Lagrangian trajectories for generators

Generators trajectories

$$\mathbf{x}_{\text{gen}}^{n+1} = \mathbf{x}_{\text{gen}}^n + \Delta t \mathbf{v}(\mathbf{x}_{\text{gen}}^n)$$

Integrated with **high order of accuracy** by a **Taylor expansion**

$$\mathbf{x}_{\text{gen}}^{n+1} = \mathbf{x}_{\text{gen}}^n + \Delta t \frac{d\mathbf{x}}{dt} + \frac{\Delta t^2}{2} \frac{d^2\mathbf{x}}{dt^2} + \frac{\Delta t^3}{6} \frac{d^3\mathbf{x}}{dt^3} + \frac{\Delta t^4}{24} \frac{d^4\mathbf{x}}{dt^4} + \mathcal{O}(5),$$

where

- **spatial derivatives** are replaced, via the *Cauchy-Kovalevskaya* procedure, using the trajectory equation

$$\frac{d\mathbf{x}}{dt} = \mathbf{v}(\mathbf{x}(t)),$$

- and \mathbf{v} is recovered from conserved variables represented through high order **modal polynomials**

Mesh optimization techniques - in brief

Ingredients

- High order Lagrangian position $\mathbf{x}_{\text{gen}}^{n+1}$
 \Rightarrow optimal in following the flow of the fluid
- $\mathbf{x}_{\mathbf{c}_i}^*$ prescribed by a smoothing technique (Lloyd-like smoothing or Laplacian smoothing) \Rightarrow optimal in the sense of mesh quality

$$\hat{\mathbf{x}}_{\text{gen}}^{n+1} = (1 - \mu) \mathbf{x}_{\text{gen}}^{n+1} + \mu \mathbf{x}_{\mathbf{c}_i}^*, \quad \text{with } \mu = \min \left(1, \sqrt{\frac{U_* \Delta t}{\Delta s} \mathcal{F}} \right)$$

- U_* maximum of fluid velocity
- Δt timestep size, Δs min of mesh size,
- \mathcal{F} nondimensional *smoothing parameter*: fixes smoothing strength

High order on Voronoi elements - Shu vortex

Euler equations: stationary rotating vortex

Domain: $[x, y] \in [-5, 5] \times [-5, 5]$

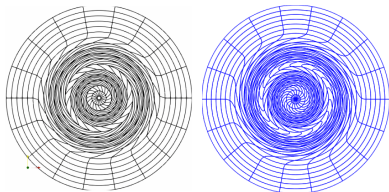
Data: $\epsilon = 5, \gamma = 1.4, r = \sqrt{x^2 + y^2}$

Initial conditions:

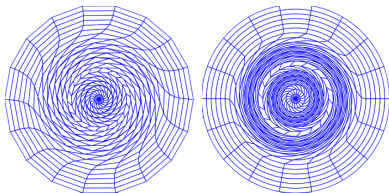
$$\begin{cases} \delta T = -\frac{(\gamma-1)\epsilon^2}{8\gamma\pi^2} e^{1-r^2} \\ \rho = 1 + d\rho, \quad \delta\rho = (1 + \delta T)^{\frac{1}{\gamma-1}} - 1 \\ u = 0 + \partial u, \quad \partial u = -y \frac{\epsilon}{2\pi} e^{\frac{1-r^2}{2}} \\ v = 0 + \partial v, \quad \partial v = x \frac{\epsilon}{2\pi} e^{\frac{1-r^2}{2}} \\ p = 1 + \partial p, \quad \delta p = (1 + \delta T)^{\frac{\gamma}{\gamma-1}} - 1 \end{cases}$$

Other Lagrangian methods dealing with vortical flows

- **Shashkov & Morgan - USA**

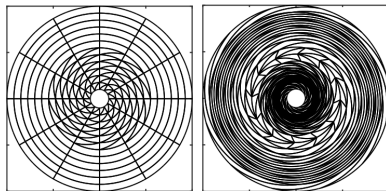


- **Maire & Vilar - CEA**

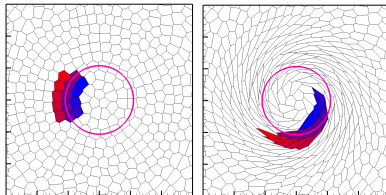


My network before top. changes

- **Standard ALE approach**



- **Standard ALE + Voronoi**



High order on Voronoi elements - Shu vortex

High order on Voronoi elements - Shu vortex

High order on Voronoi elements - Shu vortex

FV

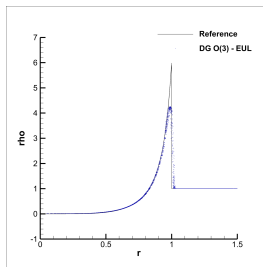
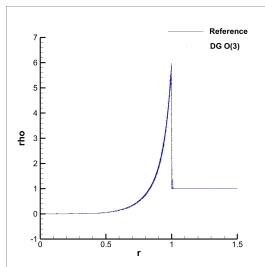
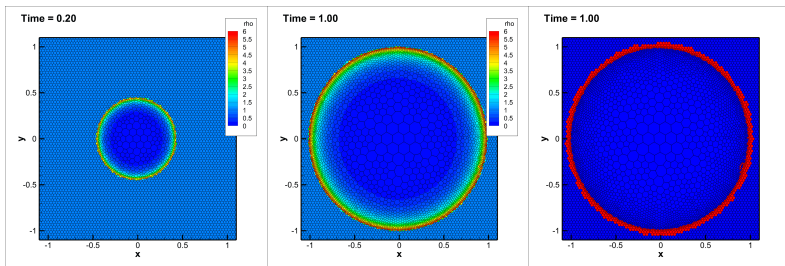
$P_0P_1 \rightarrow \mathcal{O}2$			$P_0P_2 \rightarrow \mathcal{O}3$			$P_0P_3 \rightarrow \mathcal{O}4$			$P_0P_4 \rightarrow \mathcal{O}5$		
h_f	$\epsilon(\rho)_{L_1}$	\mathcal{O}	h_f	$\epsilon(\rho)_{L_1}$	\mathcal{O}	h_f	$\epsilon(\rho)_{L_1}$	\mathcal{O}	h_f	$\epsilon(\rho)_{L_1}$	\mathcal{O}
3.8E-01	3.1E-02	-	3.8E-01	2.9E-02	-	1.9E-01	1.6E-03	-	4.7E-01	4.0e-02	-
2.0E-01	6.2E-03	2.4	1.9E-01	4.6E-03	2.8	1.3E-01	4.1E-04	3.4	3.8E-01	1.4e-02	4.8
1.3E-01	2.4E-03	2.4	1.3E-01	1.4E-03	2.9	9.9E-02	1.4E-04	3.8	1.3E-01	2.5e-04	3.8
9.9E-02	1.3E-03	2.3	9.9E-02	6.1E-04	3.0	7.9E-02	6.0E-05	3.9	9.9E-02	6.7e-05	4.6
8.0E-02	7.8E-04	2.2	7.9E-02	3.1E-04	2.0	6.7E-03	3.0E-05	3.8	7.9E-02	2.4e-05	4.7

DG

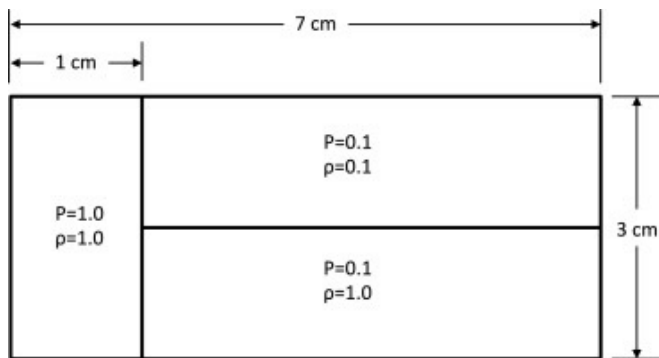
$P_1P_1 \rightarrow \mathcal{O}2$			$P_2P_2 \rightarrow \mathcal{O}3$			$P_3P_3 \rightarrow \mathcal{O}4$			$P_4P_4 \rightarrow \mathcal{O}5$		
h_f	$\epsilon(\rho)_{L_1}$	\mathcal{O}	h_f	$\epsilon(\rho)_{L_1}$	\mathcal{O}	h_f	$\epsilon(\rho)_{L_1}$	\mathcal{O}	h_f	$\epsilon(\rho)_{L_1}$	\mathcal{O}
7.5E-01	6.3E-03	-	7.5E-01	1.4E-02	-	6.1E-01	1.4E-03	-	1.4E-00	1.1e-02	-
6.1E-01	4.2E-04	1.9	6.1E-01	7.2E-03	3.4	5.2E-01	7.4E-04	3.7	1.0E-00	2.0e-03	5.9
3.2E-01	9.9E-04	2.2	3.2E-01	9.3E-04	3.2	4.7E-01	4.1E-04	5.9	9.8E-01	1.6e-03	4.7
2.2E-01	4.4E-04	2.0	2.2E-01	2.8E-04	3.0	3.2E-01	7.7E-05	4.4	8.9E-01	9.0e-04	5.9
1.6E-01	2.5E-05	2.0	1.6E-01	1.2E-04	3.0	2.2E-01	1.6E-05	4.0	8.5E-01	7.0e-04	5.1

Table: Isentropic vortex. The L_1 error norms refer to the variable ρ at time $t = 0.5$.

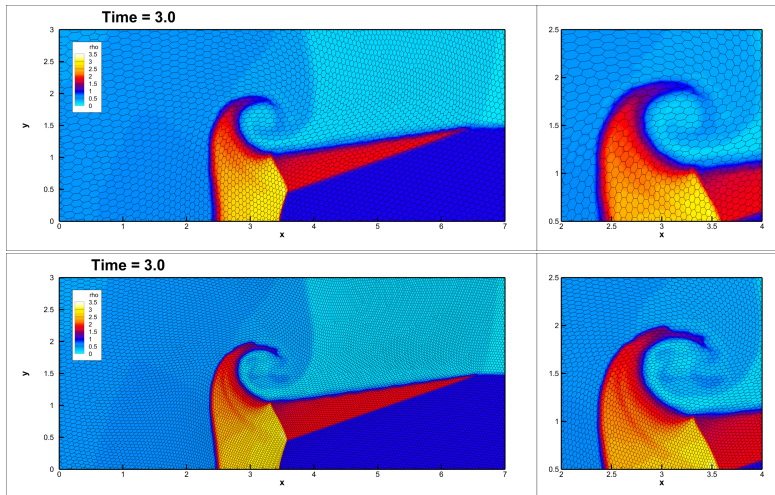
High order on Voronoi elements: Sedov test case



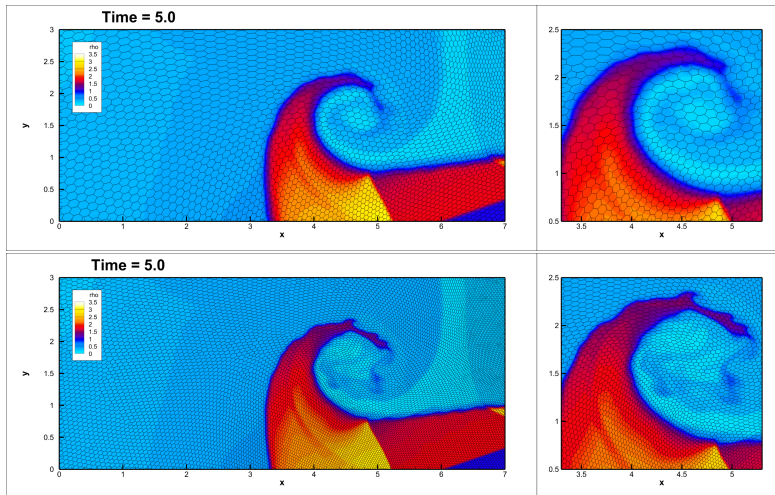
Triple point problem



Triple point problem

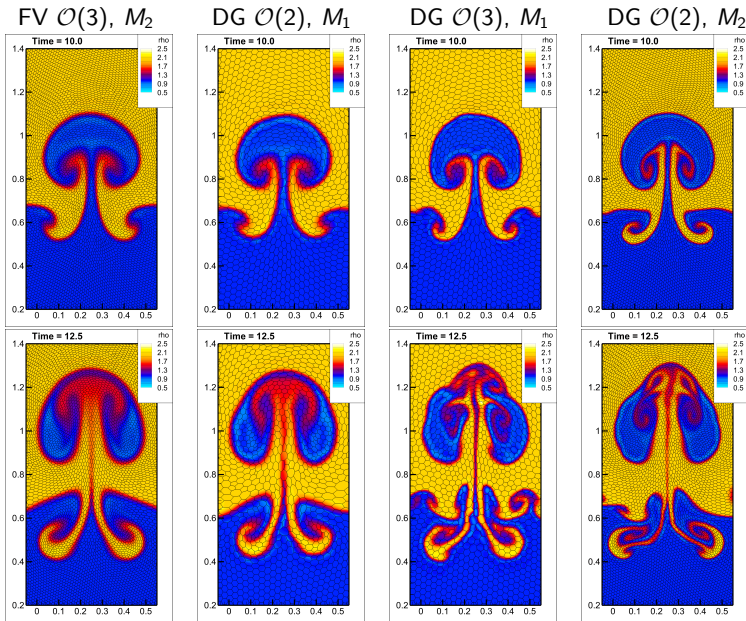


Triple point problem



Rayleigh-Taylor instability

(adding a gravity source term)



High order on Voronoi elements: MHD equations

MHD equations

$$\partial_t \mathbf{Q} + \nabla \cdot \mathbf{F}(\mathbf{Q}) = \mathbf{S}(\mathbf{Q})$$

$$\partial_t \begin{pmatrix} \rho \\ \rho u \\ \rho v \\ \rho E \\ B_x \\ B_y \\ \Phi \end{pmatrix} + \partial_x \begin{pmatrix} \rho u \\ \rho u^2 + \left(\rho + \frac{1}{8\pi} \mathbf{B}^2\right) + \frac{B_x B_x}{4\pi} \\ \rho uv - \frac{B_y B_x}{4\pi} \\ u \left(\rho E + \rho + \frac{1}{8\pi} \mathbf{B}^2\right) - \frac{B_x (\mathbf{v} \cdot \mathbf{B})}{4\pi} \\ B_x u - u B_x + \Phi \\ B_y u - v B_x \\ c_h^2 B_x \end{pmatrix} + \partial_y \begin{pmatrix} \rho v \\ \rho uv - \frac{B_y B_x}{4\pi} \\ \rho v^2 + \left(\rho + \frac{1}{8\pi} \mathbf{B}^2\right) + \frac{B_y B_y}{4\pi} \\ v \left(\rho E + \rho + \frac{1}{8\pi} \mathbf{B}^2\right) - \frac{B_y (\mathbf{v} \cdot \mathbf{B})}{4\pi} \\ B_x v - u B_y \\ B_y v - v B_y + \Phi \\ c_h^2 B_y \end{pmatrix} = \mathbf{0}$$

$$p = (\gamma - 1) \left(\rho E - \frac{1}{2} (u^2 + v^2) - \frac{\mathbf{B}^2}{8\pi} \right) = 0$$

ρ density, $\mathbf{u} = (u, v)$ velocities, p pressure, E total energy,
 \mathbf{B} magnetic field, Φ additional variable, c_h **divergence cleaning** speed

High order on Voronoi elements: smooth MHD vortex

Initial condition:

$$\mathbf{V}(\mathbf{x}, 0) = (1, 1 + \delta u, 1 + \delta v, 0, 1 + \delta p, \delta B_x, \delta B_y, \delta B_z, 0),$$

with $\delta \mathbf{v} = (\delta u, \delta v, \delta w)$, $\delta \mathbf{B} = (\delta B_x, \delta B_y, \delta B_z)$ and

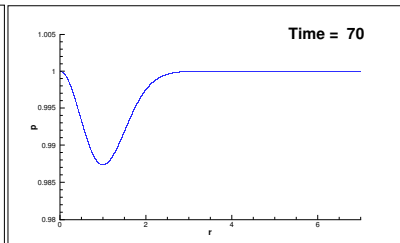
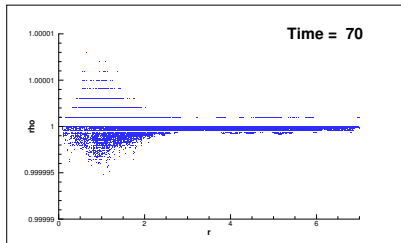
$$\delta \mathbf{v} = \frac{\kappa}{2\pi} e^{\frac{1}{2}(1-r^2)} \mathbf{e}_z \times \mathbf{r} \quad \delta \mathbf{B} = \frac{\mu}{2\pi} e^{\frac{1}{2}(1-r^2)} \mathbf{e}_z \times \mathbf{r}, \quad \delta p = \frac{1}{64q\pi^3} \left(\mu^2(1-r^2) - 4\kappa^2\pi \right) e^{(1-r^2)}$$

Data: $\mathbf{e}_z = (0, 0, 1)$, $c_h = 1$, $q = \frac{1}{2}$, $\kappa = 1$, $\mu = \sqrt{4\pi}$ **DG** 3rd order

- Statistics

Method	timesteps	slivers	restarts	Mesh%	$P_N P_M$	st%	on sliver%
DG $\mathcal{O}(4)$	62741	21369	3	0.17	97.39		7.5E-4

- Density and pressure *scatter* profiles after 3 turns



High order on Voronoi elements

FV

$P_0P_1 \rightarrow \mathcal{O}2$			$P_0P_2 \rightarrow \mathcal{O}3$			$P_0P_3 \rightarrow \mathcal{O}4$			$P_0P_4 \rightarrow \mathcal{O}5$		
h_f	$\epsilon(\rho)_{L_1}$	\mathcal{O}	h_f	$\epsilon(\rho)_{L_1}$	\mathcal{O}	h_f	$\epsilon(\rho)_{L_1}$	\mathcal{O}	h_f	$\epsilon(\rho)_{L_1}$	\mathcal{O}
4.6E-01	3.3E-02	-	3.2E-01	1.0E-02	-	4.7E-01	2.1E-02	-	6.0E-01	3.6e-02	-
3.9E-01	1.6E-02	1.8	2.4E-01	5.5E-03	2.3	3.2E-01	6.0E-03	3.2	5.8E-01	3.0e-02	5.8
2.4E-01	8.9E-03	2.3	1.9E-01	2.7E-03	3.3	2.4E-01	2.0E-03	3.9	5.6E-01	2.7e-02	3.6
1.9E-01	5.3E-03	2.4	1.6E-01	1.5E-03	3.1	2.2E-01	1.3E-03	3.6	5.5E-01	2.3e-02	5.9
1.6E-01	3.4E-03	2.5	1.4E-01	1.0E-03	2.9	1.9E-01	8.1E-04	4.8	5.2E-01	1.8e-02	4.8

DG

$P_1P_1 \rightarrow \mathcal{O}2$			$P_2P_2 \rightarrow \mathcal{O}3$			$P_3P_3 \rightarrow \mathcal{O}4$			$P_4P_4 \rightarrow \mathcal{O}5$		
h_f	$\epsilon(\rho)_{L_1}$	\mathcal{O}	h_f	$\epsilon(\rho)_{L_1}$	\mathcal{O}	h_f	$\epsilon(\rho)_{L_1}$	\mathcal{O}	h_f	$\epsilon(\rho)_{L_1}$	\mathcal{O}
4.7E-01	8.5E-03	-	6.1E-01	2.8E-03	-	8.8E-01	1.1E-03	-	1.6E-00	6.9e-03	-
3.2E-01	3.2E-04	2.5	4.7E-01	1.3E-03	2.8	7.5E-01	6.2E-04	3.5	6.1E-01	1.3e-04	4.1
2.8E-01	2.1E-04	2.9	3.8E-01	7.3E-04	2.7	6.1E-01	3.1E-04	3.4	5.2E-01	4.7e-05	5.8
2.4E-01	1.6E-04	2.0	3.5E-01	5.6E-04	3.6	5.5E-01	1.9E-04	4.3	4.9E-01	3.1e-05	8.1
1.9E-01	9.7E-05	2.4	3.2E-01	4.1E-04	3.0	3.2E-01	2.3E-05	3.9	4.7E-01	2.4e-05	5.3

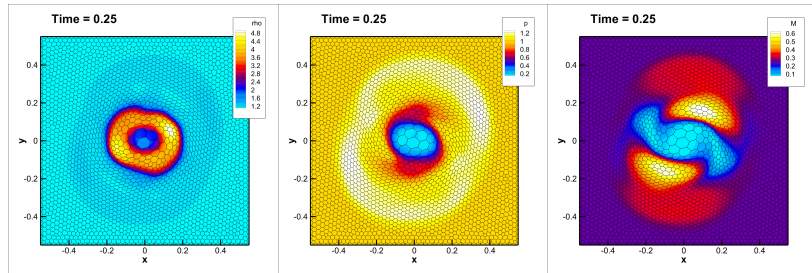
Table: MHD vortex. The L_1 error norms refer to the variable ρ at time $t = 1.0$.

MHD rotor problem

Rapidly rotating fluid of high density embedded in a fluid at rest with low density, both subject to an initially constant magnetic field

$$\text{IC: } \begin{cases} \rho = 10, \omega = 10 & \text{if } 0 \leq r \leq 0.1 \\ \rho = 1, \omega = 0 & \text{otherwise} \\ P = 1 \\ \mathbf{B} = (2.5, 0, 0) & t_f = 0.25 \end{cases}$$

FV $\mathcal{O}(4)$, P_0P_3 , coarse

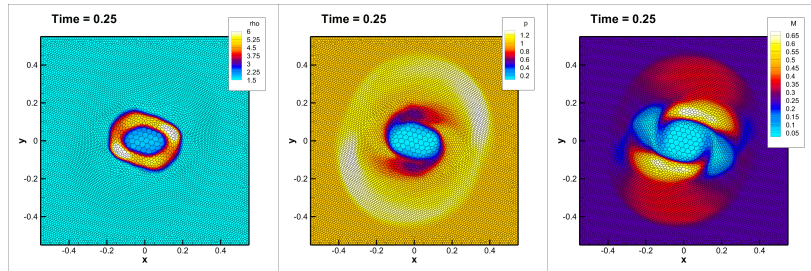


MHD rotor problem

Rapidly rotating fluid of high density embedded in a fluid at rest with low density, both subject to an initially constant magnetic field

$$\text{IC : } \begin{cases} \rho = 10, \omega = 10 & \text{if } 0 \leq r \leq 0.1 \\ \rho = 1, \omega = 0 & \text{otherwise} \\ P = 1 \\ \mathbf{B} = (2.5, 0, 0) & t_f = 0.25 \end{cases}$$

FV $\mathcal{O}(4)$, P_0P_3 , fine

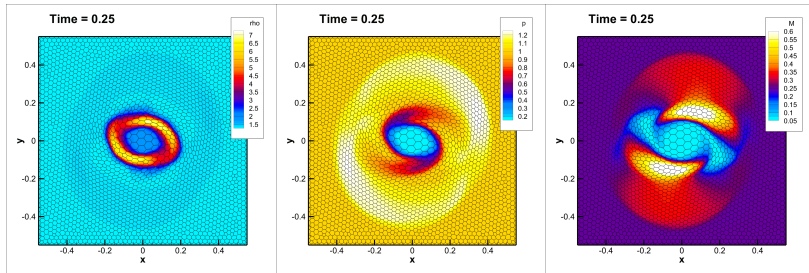


MHD rotor problem

Rapidly rotating fluid of high density embedded in a fluid at rest with low density, both subject to an initially constant magnetic field

$$\text{IC : } \begin{cases} \rho = 10, \omega = 10 & \text{if } 0 \leq r \leq 0.1 \\ \rho = 1, \omega = 0 & \text{otherwise} \\ P = 1 \\ \mathbf{B} = (2.5, 0, 0) & t_f = 0.25 \end{cases}$$

DG $\mathcal{O}(3)$, P_2P_2 , coarse

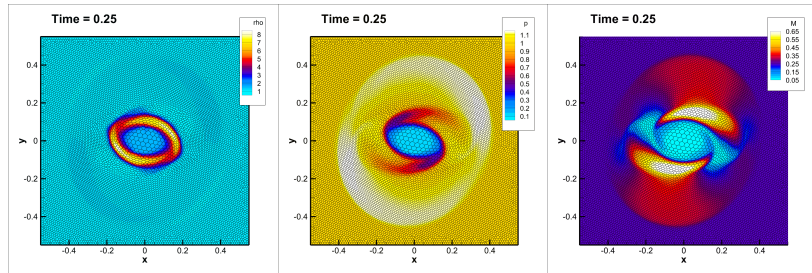


MHD rotor problem

Rapidly rotating fluid of high density embedded in a fluid at rest with low density, both subject to an initially constant magnetic field

$$\text{IC : } \begin{cases} \rho = 10, \omega = 10 & \text{if } 0 \leq r \leq 0.1 \\ \rho = 1, \omega = 0 & \text{otherwise} \\ P = 1 \\ \mathbf{B} = (2.5, 0, 0) & t_f = 0.25 \end{cases}$$

DG $\mathcal{O}(3)$, P_2P_2 , fine



Direct ALE FV scheme with nonconservative products

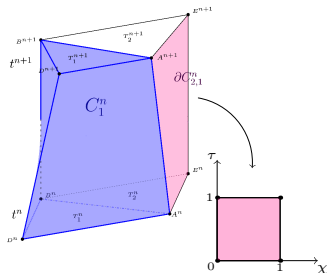
ALE FV-DG scheme

$$\int_{\partial C_i^n} (\tilde{\mathbf{F}} + \tilde{\mathbf{D}}) \cdot \tilde{\mathbf{n}} + \int_{C_i^n \setminus \partial C_i^n} \tilde{\mathbf{B}} \cdot \tilde{\nabla} \mathbf{Q} = \int_{C_i^n} \mathbf{S}$$

$$\int_{T_i^{n+1}} \mathbf{Q}_i^{n+1} = \int_{T_i^n} \mathbf{Q}_i^n - \int_{\partial C_i^n} \mathcal{F} + \mathcal{D}(\mathbf{q}_h^-, \mathbf{q}_h^+) \cdot \tilde{\mathbf{n}}$$

$$+ \int_{C_i^n} \tilde{\mathbf{B}}(\mathbf{q}_h) \cdot \tilde{\nabla} \mathbf{Q}(\mathbf{q}_h)$$

$$+ \int_{C_i^n} \tilde{\mathbf{S}}(\mathbf{q}_h)$$



ALE numerical flux: nonconservative part

$\mathcal{F} + \mathcal{D}(\mathbf{q}_h^-, \mathbf{q}_h^+) \cdot \tilde{\mathbf{n}}$ represents the well balanced ALE numerical flux between two neighbors across ∂C_{ij}^n

Osher-type ALE scheme

$$\begin{aligned} (\tilde{\mathbf{F}}_{ij} + \tilde{\mathbf{D}}_{ij}) \cdot \tilde{\mathbf{n}}_{ij} &= \frac{1}{2} \left(\tilde{\mathbf{F}}(\mathbf{q}_h^+) + \tilde{\mathbf{F}}(\mathbf{q}_h^-) + \mathcal{D}(\mathbf{q}_h^+ - \mathbf{q}_h^-) \right) \cdot \tilde{\mathbf{n}}_{ij} \\ &\quad - \frac{1}{2} \left(\int_0^1 \left| \mathbf{A}_n^V(\Psi(s)) \right| ds \right) (\mathbf{q}_h^+ - \mathbf{q}_h^-) \end{aligned}$$

- $\mathcal{D}(\mathbf{q}_h^+ - \mathbf{q}_h^-)$: well balanced way to write the nonconservative terms
- $\mathbf{A}_n^V(\mathbf{Q})$ is the **extended ALE Jacobian matrix**

$$\mathbf{A}_n^V(\mathbf{Q}) = \left(\sqrt{\tilde{n}_x^2 + \tilde{n}_y^2} \right) \left[\left(\frac{\partial \mathbf{F}}{\partial \mathbf{Q}} + \mathbf{B} \right) \cdot \mathbf{n} - (\mathbf{V} \cdot \mathbf{n}) \mathbf{I} \right], \quad \mathbf{n} = \frac{(\tilde{n}_x, \tilde{n}_y)^T}{\sqrt{\tilde{n}_x^2 + \tilde{n}_y^2}}$$

$\mathcal{F} + \mathcal{D}$ defined in terms of a **family of paths** $\Phi(s, \mathbf{q}^-, \mathbf{q}^+)$, $s \in [0, 1]$.

- According to [3], Lipschitz continuous family of paths $\Phi(s, \mathbf{q}^-, \mathbf{q}^+)$, $s \in [0, 1]$ satisfying

$$\Phi(0, \mathbf{q}^-, \mathbf{q}^+) = \mathbf{q}^-, \quad \Phi(1, \mathbf{q}^-, \mathbf{q}^+) = \mathbf{q}^+, \quad \Phi(s, \mathbf{q}, \mathbf{q}) = \mathbf{q},$$

and $\mathcal{D}(\mathbf{q}^+ - \mathbf{q}^-) \simeq \int_0^1 \mathbf{B}(\Phi(s; \mathbf{q}^-, \mathbf{q}^+)) \frac{\partial \Phi}{\partial s}(s; \mathbf{q}^-, \mathbf{q}^+) ds$

[3] G. Dal Maso and P.G. LeFloch and F. Murat, J. Math. Pures Appl., 1995,

[2] C. Parés, SIAM Journal on Numerical Analysis, 2006

$\mathcal{F} + \mathcal{D}$ defined in terms of a **family of paths** $\Phi(s, \mathbf{q}^-, \mathbf{q}^+)$, $s \in [0, 1]$.

- According to [3], Lipschitz continuous family of paths $\Phi(s, \mathbf{q}^-, \mathbf{q}^+)$, $s \in [0, 1]$ satisfying

$$\Phi(0, \mathbf{q}^-, \mathbf{q}^+) = \mathbf{q}^-, \quad \Phi(1, \mathbf{q}^-, \mathbf{q}^+) = \mathbf{q}^+, \quad \Phi(s, \mathbf{q}, \mathbf{q}) = \mathbf{q},$$

and $\mathcal{D}(\mathbf{q}^+ - \mathbf{q}^-) \simeq \int_0^1 \mathbf{B}(\Phi(s; \mathbf{q}^-, \mathbf{q}^+)) \frac{\partial \Phi}{\partial s}(s; \mathbf{q}^-, \mathbf{q}^+) ds$

- According to [2]:

A sufficient condition for a well balanced scheme

$$\left(\tilde{\mathbf{F}}_{ij} + \tilde{\mathbf{D}}_{ij} \right) (\mathbf{q}_E^-, \mathbf{q}_E^+) = \mathbf{0}, \text{ if } \mathbf{q}_E^- \text{ and } \mathbf{q}_E^+ \text{ lie on the same stationary sol}$$

[3] G. Dal Maso and P.G. LeFloch and F. Murat, J. Math. Pures Appl., 1995,

[2] C. Parés, SIAM Journal on Numerical Analysis, 2006

Well balanced path

Standard path (segment): $\Phi(s; \mathbf{q}^-, \mathbf{q}^+) = \mathbf{q}^- + s(\mathbf{q}^+ - \mathbf{q}^-)$
 2^{nd} order accurate, but not well balanced for general profiles

Well balanced path

Standard path (segment): $\Phi(s; \mathbf{q}^-, \mathbf{q}^+) = \mathbf{q}^- + s(\mathbf{q}^+ - \mathbf{q}^-)$
 2^{nd} order accurate, but not well balanced for general profiles

Proposed path: equilibrium + fluctuation

$$\Phi(s, \mathbf{q}^-, \mathbf{q}^+) = \Phi^E(s, \mathbf{q}_E^-, \mathbf{q}_E^+) + \Phi^f(s, \mathbf{q}_f^-, \mathbf{q}_f^+)$$

- $\Phi^E(s, \mathbf{q}_E^-, \mathbf{q}_E^+)$ reparametrization of the stationary solution that connects the state \mathbf{q}_E^- with \mathbf{q}_E^+
- $\mathbf{q}_f^- = \mathbf{q}^- - \mathbf{q}_E^-$ and $\mathbf{q}_f^+ = \mathbf{q}^+ - \mathbf{q}_E^+$
- $\Phi^f(s, \mathbf{q}_f^-, \mathbf{q}_f^+) = \mathbf{q}_f^- + s(\mathbf{q}_f^+ - \mathbf{q}_f^-)$

2nd order well balanced reconstruction

MUSCL-Hancock method

$$\mathcal{P}_i(x, t) = \mathbf{Q}_i^n + \frac{\Delta \mathbf{Q}_i^n}{\Delta x} (x - x_i) + \partial_t \mathbf{Q}_i (t - t^n)$$

We introduce a reconstructor operator defined as

$$\mathbf{Q}_i^n(x, t) = \mathbf{Q}^E_i(x, t) + \mathcal{P}^f_i(x, t), \quad x \in I_i, \quad t \in [t^n, t^{n+1}]$$

- \mathbf{Q}^E Smooth stationary solution
- \mathcal{P}^f Standard reconstruction operator over the fluctuations

Euler equations with gravity

Euler equations of gasdynamics with gravity - Polar coordinates

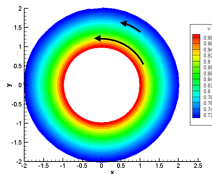
$$\partial_t \mathbf{Q} + \nabla \cdot \mathbf{F}(\mathbf{Q}) = \mathbf{S}(\mathbf{Q})$$

$$\partial_t \begin{pmatrix} r\rho \\ r\rho u \\ r\rho v \\ r\rho E \end{pmatrix} + \partial_r \begin{pmatrix} r\rho u \\ r\rho u^2 + rP \\ r\rho uv \\ ru(\rho E + P) \end{pmatrix} + \partial_y \begin{pmatrix} \rho v \\ \rho uv \\ \rho v^2 + P \\ v(\rho E + P) \end{pmatrix} = \begin{pmatrix} 0 \\ -\rho \frac{Gm_s}{r} + P + \rho v^2 \\ -\rho uv \\ -\rho u \frac{Gm_s}{r} \end{pmatrix}$$

Equilibrium properties:

$$u = 0, \quad \frac{\partial v}{\partial y} = 0,$$

$$r \frac{\partial P}{\partial r} + \rho \left(\frac{Gm_s}{r} - \rho v^2 \right) = 0$$



High shear flow

Nonconservative system

$$\partial_t \mathbf{Q} + \nabla \cdot \mathbf{F}(\mathbf{Q}) + \mathbf{B}(\mathbf{Q}) \cdot \nabla \mathbf{Q} = \mathbf{0}$$

+ path-conservative scheme with a *particular* path

Euler equations of gasdynamics with gravity - polar coordinates

$$\partial_t \mathbf{Q} + \nabla \cdot \mathbf{F}(\mathbf{Q}) + \mathbf{B}(\mathbf{Q}) \cdot \nabla \mathbf{Q} = \mathbf{S}(\mathbf{Q})$$

$$\partial_t \begin{pmatrix} r\rho \\ r\rho u \\ r\rho v \\ r\rho E \\ r \end{pmatrix} + \partial_r \begin{pmatrix} r\rho u \\ r\rho u^2 \\ r\rho uv \\ ru(\rho E + P) \\ 0 \end{pmatrix} + \partial_y \begin{pmatrix} \rho v \\ \rho uv \\ \rho v^2 + P \\ v(\rho E + P) \\ 0 \end{pmatrix} + \begin{pmatrix} 0 \\ r \frac{\partial P}{\partial r} + \rho \left(\frac{Gm_s}{r} - v^2 \right) \frac{\partial r}{\partial r} \\ \rho uv \frac{\partial r}{\partial r} \\ \rho u \frac{Gm_s}{r} \frac{\partial r}{\partial r} \\ 0 \end{pmatrix} = \mathbf{0}$$

$r \rightarrow$ radial direction, $y \rightarrow$ angular direction
 $u \rightarrow$ radial velocity, $v \rightarrow$ angular velocity

$$\frac{\partial r}{\partial t} = 0 \quad \frac{\partial r}{\partial r} = 1$$

WB for Euler equations with gravity

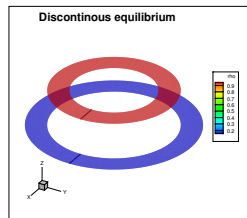
2d Equilibrium - up to machine precision

Domain: $[r, \varphi] \in [1, 2] \times [0, 2\pi]$

Data: $r_m = 1.5, G = 1, m_s = 1$

Initial conditions:

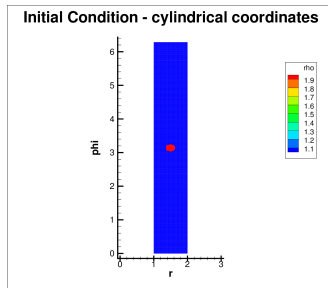
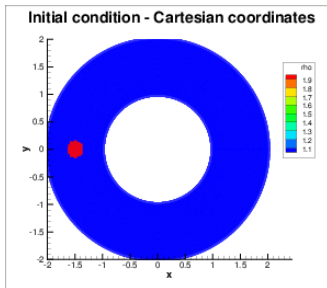
$$\begin{cases} \rho = 1, & \text{if } r < r_m, \\ \rho = 0.1, & \text{if } r \geq r_m, \\ u = 0 \\ v = \sqrt{\frac{Gm_s}{r}} \\ P = 1 \end{cases}$$



points 20×40		
time	$\mathcal{O}1$	$\mathcal{O}2$
10	7.32E-13	4.20E-13
40	2.83E-12	8.18E-12
80	3.92E-12	1.72E-11
100	2.25E-12	1.99E-11

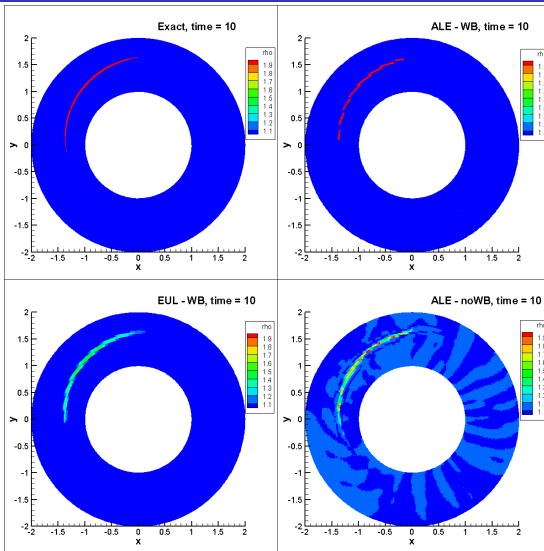
Keplerian disk: transport of a higher density quantity

Equilibrium $\rho_E = 1, u_E = 0, v_E = \sqrt{\frac{Gms}{r}}, P = 1$
Perturbation $\rho = 2$ in $(x - 1.5)^2 + y^2 \leq (0.15)^2$



Keplerian disk: transport of a higher density quantity

Keplerian disk: transport of a higher density quantity



Kelvin-Helmholtz instabilities

Equilibrium

$$\begin{cases} \rho_E = \rho_0 + \rho_1 \tanh\left(\frac{r-r_m}{\sigma}\right) \\ u_E = 0 \\ v_E = \sqrt{\frac{Gm_s}{r}} \\ \rho_E = 1 \end{cases}$$

Parameters:

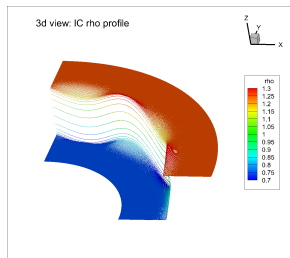
$G = 1$, $m_s = 1$, $\rho_0 = 1$, $\rho_1 = 0.25$,
 $r_m = 1.5$ and $\sigma = 0.01$

Domain: ring sector $r \in [1, 2]$, $\varphi \in [0, \pi/2]$

Boundary conditions:

exact solution $r = 1, 2$

periodic boundary conditions $\varphi = 0, \pi/2$.

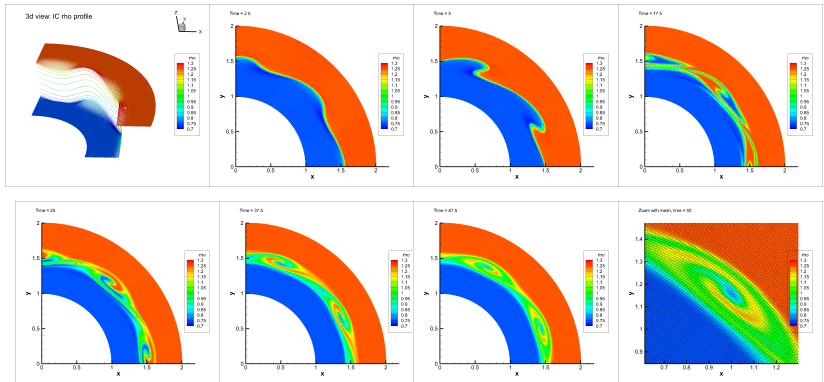


Initial condition:

$$\begin{cases} \rho = \rho_E + A \rho_0 \sin(k\varphi) \exp\left(-\frac{(r-r_m)^2}{s}\right) \\ u = u_E + A \sin(k\varphi) \exp\left(-\frac{(r-r_m)^2}{s}\right) \\ v = v_E \\ p = p_E + A \sin(k\varphi) \exp\left(-\frac{(r-r_m)^2}{s}\right) \end{cases}$$

with $A = 0.1$, $k = 8$, $s = 0.005$

Our Well Balanced ALE FV Osher-Romberg scheme

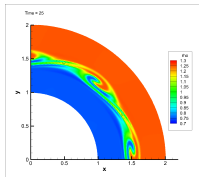


Well-balanced Arbitrary-Lagrangian-Eulerian finite volume schemes on moving nonconforming meshes for the Euler equations of gas dynamics with gravity

Publication: E. Gaburro, M.J. Castro, M. Dumbser, MNRAS (2018)

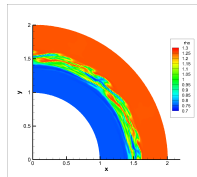
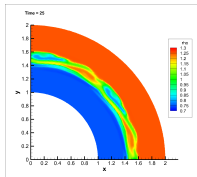
Kelvin-Helmholtz instabilities - comparison

Ours

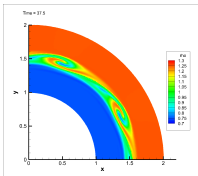


vs

not WB - not ALE:

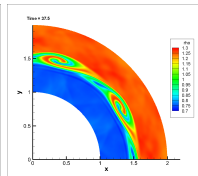
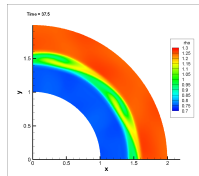
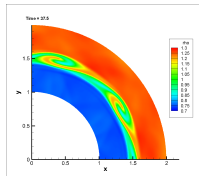


Ours



vs

PLUTO:



GRMHD: general relativistic magnetohydrodynamics

$$\partial_t \mathbf{Q} + \nabla \cdot \mathbf{F}(\mathbf{Q}) + \mathbf{B}(\mathbf{Q}) \cdot \nabla \mathbf{Q} = 0$$

$$\mathbf{V} := (\rho, v_j, p, B^j, \Phi, \alpha, \beta^j, \tilde{\gamma}_m), \quad j = 1, 2, 3; \quad m = 1, \dots, 6,$$

$$\mathbf{Q} := (\sqrt{\gamma} D, \sqrt{\gamma} S_j, \sqrt{\gamma} \tau, \sqrt{\gamma} B^j, \Phi, \alpha, \beta^j, \tilde{\gamma}_m)$$

$$\mathbf{F} := \gamma^{\frac{1}{2}} \begin{pmatrix} \alpha v^i D - \beta^i D \\ \alpha T_j^i - \beta^i S_j \\ \alpha (S^i - v^i D) - \beta^i \tau \\ (\alpha v^i - \beta^i) B^j - (\alpha v^j - \beta^j) B^i \\ 0 \\ 0 \\ 0 \\ 0 \end{pmatrix}, \quad \mathbf{B}(\mathbf{Q}) \cdot \nabla \mathbf{Q} := \begin{pmatrix} 0 \\ \gamma^{\frac{1}{2}} (U \partial_j \alpha - \frac{1}{2} \alpha T^{ik} \partial_j \gamma_{ik} - S_i \partial_j \beta^i) \\ \gamma^{\frac{1}{2}} (S^j \partial_j \alpha - \frac{1}{2} T^{ik} \beta^j \partial_j \gamma_{ik} - T_i^j \partial_j \beta^i) \\ -\beta^j \partial_i (\gamma^{\frac{1}{2}} B^i) + \alpha \gamma^{\frac{1}{2}} \gamma^{ji} \partial_i \Phi \\ \gamma^{-\frac{1}{2}} \alpha c_h^2 \partial_j (\gamma^{\frac{1}{2}} B^j) - \beta^j \partial_j \Phi \\ 0 \\ 0 \\ 0 \end{pmatrix}$$

Publication:  Fambri, Dumbser, Köppel, Rezzolla, Zanotti, MNRAS 2018

CCZ4: Einstein field equations (hyp. order 1, 59 eq.)

$$\begin{aligned}
 \partial_t \tilde{\gamma}_{ij} &= \beta^k 2D_{kij} + \tilde{\gamma}_{ki} B_j^k + \tilde{\gamma}_{kj} B_i^k - 2/3 \tilde{\gamma}_{ij} B_k^k - 2\alpha \left(\tilde{A}_{ij} - 1/3 \tilde{\gamma}_{ij} \text{tr} \tilde{A} \right) - \tau^{-1} (\tilde{\gamma} - 1) \tilde{\gamma}_{ij}, \\
 \partial_t \ln \alpha &= \beta^k A_k - \alpha g(\alpha) (K - K_0 - 2\Theta c), \\
 \partial_t \beta^i &= s \beta^k B_k^i + s f b^i \\
 \partial_t \ln \varphi &= \beta^k P_k + 1/3 \left(\alpha K - B_k^k \right), \\
 \partial_t \tilde{A}_{ij} - \beta^k \partial_k \tilde{A}_{ij} &- \varphi^2 \left[-\nabla_i \nabla_j \alpha + \alpha \left(R_{ij} + \nabla_i Z_j + \nabla_j Z_i \right) \right] + \varphi^2 1/3 \frac{\tilde{\gamma}_{ij}}{\varphi^2} \left[-\nabla^k \nabla_k \alpha + \alpha \left(R + 2\nabla_k Z^k \right) \right] \\
 &= \tilde{A}_{ki} B_j^k + \tilde{A}_{kj} B_i^k - 2/3 \tilde{A}_{ij} B_k^k + \alpha \tilde{A}_{ij} (K - 2\Theta c) - 2\alpha \tilde{A}_{il} \tilde{\gamma}^{lm} \tilde{A}_{mj} - \tau^{-1} \tilde{\gamma}_{ij} \text{tr} \tilde{A}, \\
 \partial_t K - \beta^k \partial_k K &+ \nabla^i \nabla_i \alpha - \alpha (R + 2\nabla_i Z^i) = \alpha K (K - 2\Theta c) - 3\alpha \kappa_1 (1 + \kappa_2) \Theta \\
 \partial_t \Theta - \beta^k \partial_k \Theta &- 1/2 \alpha e^2 (R + 2\nabla_i Z^i) = 1/2 \alpha e^2 \left(2/3 K^2 - \tilde{A}_{ij} \tilde{A}^{ij} \right) - \alpha \Theta K c - Z^i \alpha A_i - \alpha \kappa_1 (2 + \kappa_2) \Theta, \\
 \partial_t \tilde{\Gamma}^i - \beta^k \partial_k \tilde{\Gamma}^i &+ 4/3 \alpha \tilde{\gamma}^{ij} \partial_j K - 2\alpha \tilde{\gamma}^{ki} \partial_k \Theta - s \tilde{\gamma}^{kl} \partial_{(k} B_{l)}^i - s 1/3 \tilde{\gamma}^{ik} \partial_{(k} B_{l)}^j - s 2\alpha \tilde{\gamma}^{ik} \tilde{\gamma}^{nm} \partial_k \tilde{A}_{nm} \\
 &= 2/3 \tilde{\Gamma}^i B_k^k - \tilde{\Gamma}^k B_i^k + 2\alpha \left(\tilde{\Gamma}^i_{jk} \tilde{A}^{jk} - 3\tilde{A}^{ij} P_j \right) - 2\alpha \tilde{\gamma}^{ki} (\Theta A_k + 2/3 K Z_k) - 2\alpha \tilde{A}^{ij} A_j \\
 &\quad - 4s \alpha \tilde{\gamma}^{ik} D_k^{nm} \tilde{A}_{nm} + 2\kappa_3 \left(2/3 \tilde{\gamma}^{ij} Z_j B_k^k - \tilde{\gamma}^{jk} Z_j B_k^i \right) - 2\alpha \kappa_1 \tilde{\gamma}^{ij} Z_j \\
 \partial_t b^i - s \beta^k \partial_k b^i &= s \left(\partial_t \tilde{\Gamma}^i - \beta^k \partial_k \tilde{\Gamma}^i - \eta b^i \right),
 \end{aligned}$$

with the following PDEs for the auxiliary variables

$$\begin{aligned}
 \partial_t A_k - \beta^l \partial_l A_k &+ \alpha g(\alpha) (\partial_k K - \partial_k K_0 - 2c \partial_k \Theta) + s \alpha g(\alpha) \tilde{\gamma}^{nm} \partial_k \tilde{A}_{nm} \\
 &= + 2s \alpha g(\alpha) D_k^{nm} \tilde{A}_{nm} - \alpha A_k (K - K_0 - 2\Theta c) \left(g(\alpha) + \alpha g'(\alpha) \right) + B_k^l A_l, \\
 \partial_t B_k^i - s \beta^l \partial_l B_k^i &- s \left(f \partial_k b^i + \alpha^2 \mu \tilde{\gamma}^{ij} (\partial_k P_j - \partial_j P_k) - \alpha^2 \mu \tilde{\gamma}^{ij} \tilde{\gamma}^{nl} (\partial_k D_{ljn} - \partial_l D_{kjn}) \right) = s B_k^l B_l^i, \\
 \partial_t D_{kij} - \beta^l \partial_l D_{kij} &+ s \left(-1/2 \tilde{\gamma}_{mi} \partial_{(k} B_{j)}^m - 1/2 \tilde{\gamma}_{mj} \partial_{(k} B_{i)}^m + 1/3 \tilde{\gamma}_{ij} \partial_{(k} B_{m)}^m \right) + \alpha \partial_k \tilde{A}_{ij} - \alpha 1/3 \tilde{\gamma}_{ij} \tilde{\gamma}^{nm} \partial_k \tilde{A}_{nm} \\
 &= B_k^l D_{lij} + B_j^l D_{kli} + B_i^l D_{klj} - 2/3 B_l^i D_{kij} - \alpha 2/3 \tilde{\gamma}_{ij} D_k^{nm} \tilde{A}_{nm} - \alpha A_k \left(\tilde{A}_{ij} - 1/3 \tilde{\gamma}_{ij} \text{tr} \tilde{A} \right), \\
 \partial_t P_k - \beta^l \partial_l P_k &- 1/3 \alpha \partial_k K + s 1/3 \partial_{(k} B_{i)}^j - s 1/3 \alpha \tilde{\gamma}^{nm} \partial_k \tilde{A}_{nm} \\
 &= 1/3 \alpha A_k K + B_k^l P_l - s 2/3 \alpha D_k^{nm} \tilde{A}_{nm}.
 \end{aligned}$$

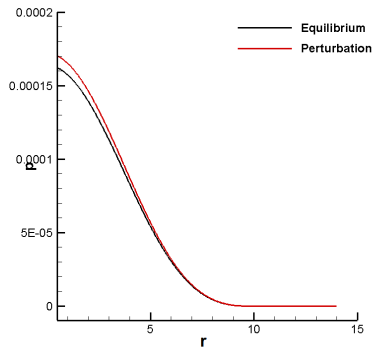
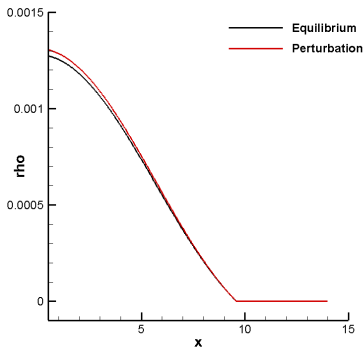
Publication:  Dumbser, Fambri, Gaburro, Reinarz, J. Comput. Phys. 2020

WB for GRMHD - TOV neutron star

Equilibrium: numerical solution of the
Tolman-Oppenheimer-Volkoff (TOV) equation

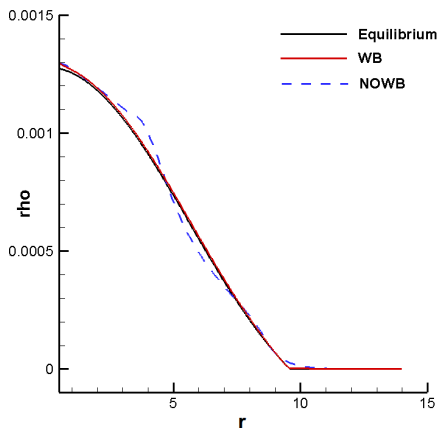
Perturbation of the order of $5e-2$ on density and pressure

Initial condition:



WB for GRMHD - TOV neutron star

Numerical results: **WB** vs **NOWB** at time = 10 000

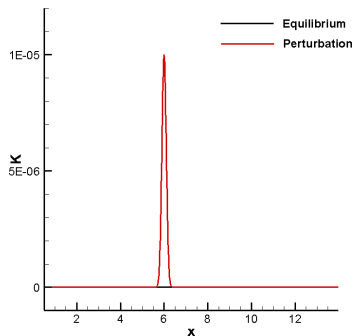


WB for CCZ4 anticowling - TOV star

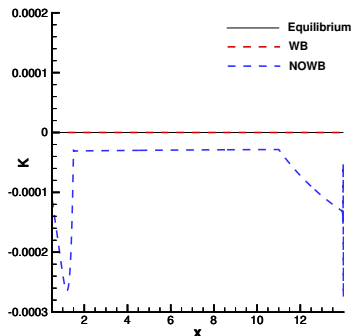
Equilibrium numerical solution of the
Tolman-Oppenheimer-Volkoff (TOV) equation

Gaussian type **perturbation** on the metric variable K (extrinsic curvature)

$t = 0$



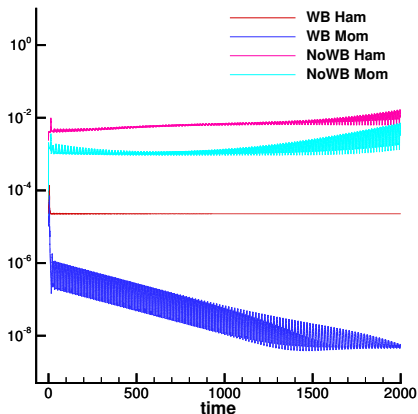
$t = 1000$



WB for CCZ4 anticowling - TOV star

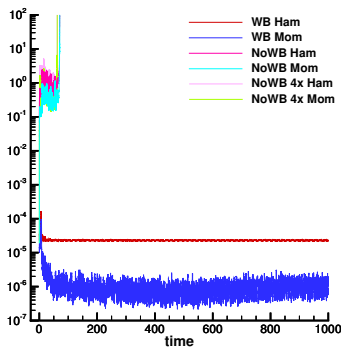
Hamiltonian constraint $\mathcal{H} = R_{ij}g^{ij} - K_{ij}K^{ij} + K^2 - 16\pi\tau = 0$

Momentum constraints $\mathcal{M}_i = \gamma^{jl} (\partial_l K_{ij} - \partial_i K_{jl} - \Gamma_{j,l}^m K_{mi} + \Gamma_{ji}^m K_{ml}) - 8\pi S_i = 0$

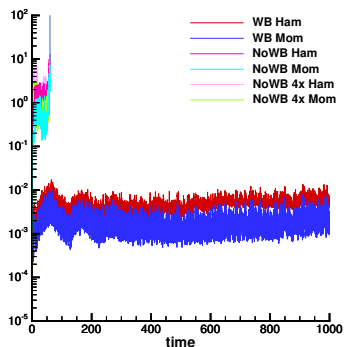


WB for CCZ4+GRHD - constraints preservation

Left: perturbation on K

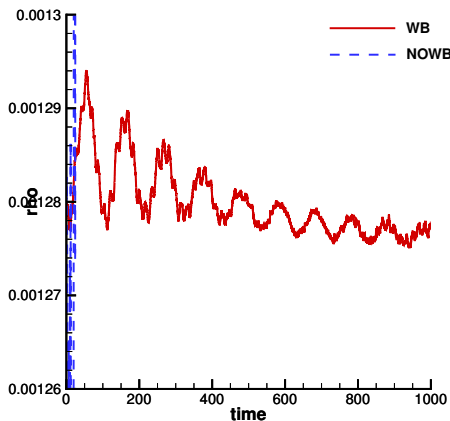


Right: perturbation on ρ



WB for CCZ4+GRMHD

Pulsation of star density at its centre subject to an initial pressure perturbation



Conclusion & Outlooks

Up to now ...

Robust arbitrary high order WB ALE FV-DG on high quality moving meshes

- Application to complex hyperbolic systems
- Low dissipation high efficiency

To be done ...

- **Moving code**: complex boundary condition (moving, periodic ...) extension to 3D of topology changes techniques
- Well balanced 3D code for **general relativity in covariant form**
- **Coupling** ALE + WB for general relativity

Thank you for your attention!

A unified framework for the solution of hyperbolic PDE systems using high order direct Arbitrary-Lagrangian-Eulerian schemes on moving unstructured meshes with topology change

E. Gaburro, Archives of Computational Methods in Engineering (2020).

High order direct ALE schemes on moving Voronoi meshes with topology changes

E. Gaburro, W. Boscheri, S. Chiocchetti, C. Klingenberg, V. Springel, M.Dumbser, JCP (2020).

Well-balanced Arbitrary-Lagrangian-Eulerian finite volume schemes on moving nonconforming meshes for the Euler equations of gas dynamics with gravity

E. Gaburro, M.J. Castro, M. Dumbser, MNRAS (2018).

Direct ALE finite volume schemes on moving nonconforming unstructured meshes

E. Gaburro, M. Dumbser, M.J. Castro, Computers & Fluids (2017).